FOR ONLINE PUBLICATION ONLY

APPENDICES

Appendix A. Biome-BGC spatial modeling and disturbance mapping

Spatial modeling. We ran the Biome-BGC model spatially at a 1 km resolution but with sub-km characterization of landcover and disturbance history, which were mapped at Landsat resolution (see below). The five most frequent combinations of cover type and disturbance history in each 1 km simulation cell were run as separate simulations, and the area-weighted mean of the five combinations was assigned to the 1 km cell. This approach resulted in approximately 90% coverage in greater than 80% of 1 km cells, which represented 395 unique combinations of landcover and disturbance history (Meigs 2009). Following model spin-up, we simulated all disturbance scenarios to the year 2004 (last year of available DAYMET climate data; see below). The primary spatial outputs were annual 1 km resolution maps of carbon pools, emissions, and net ecosystem production (NEP). Annual NEP was computed as the difference between net primary production and heterotrophic respiration (Chapin and others 2006).

We developed landcover, soil, and climate inputs using the same procedures as Turner and others (2007). Landcover was grouped into seven classes determined from two primary sources: conifer, deciduous, shrub, grass, crop, and unvegetated from the National Land Cover Data set (Vogelmann and others 2001) and *Juniperus* woodland from the Oregon GAP analysis (Kagan and others 1999). We identified the East Cascades and Cascade Crest Ecoregions from level III and level IV ecoregion descriptions, respectively (Omernik 1987; Griffith and Omernik 2009), and soil texture and depth from U.S. Geological Survey coverages (CONUS 2009). We used daily, 1 km resolution minimum and

maximum temperature, precipitation, humidity, and solar radiation data from 1980 to 2004 (Thornton and others 1997; DAYMET 2009), recycling the 25-year period during model spin-up. Landsat-derived variables (native resolution ~ 30m) were resampled to 25 m resolution and aggregated to 1 km resolution to match the scale of the climate data, and all spatial data were projected in Albers conic equal area NAD 83.

To minimize bias in the age-specific patterns of live wood mass, we ran an ecoregion-specific parameter optimization procedure with USDA Forest Service Forest Inventory and Analysis (FIA) field data (Hudiburg and others 2009) to determine the fraction of leaf nitrogen as rubisco (FLNR) and annual mortality (%) that best simulated plot-level live wood mass observations at the ecoregion scale. Specifically, we tested a range of possible parameter values with stand age based on FIA observations and a cost function based on live wood mass at the time of FIA measurements. FLNR has been used previously in optimization exercises with Biome-BGC because modeled NPP is sensitive to it, and its value is poorly constrained by measurements (White and others 2000**;** Thornton and others 2002). Mortality is likewise poorly constrained and has a strong influence on age-specific wood mass.

Disturbance mapping. In each simulation cell, we accounted for up to two disturbance events, using change detection maps for recent disturbance (since 1985) and a stand age map (Duane and others 2010) for earlier stand-replacement disturbance. For recent disturbance, we used the MTBS database (http://mtbs.gov/) for all large fires and LandTrendr change detection for stand-replacement timber harvest (Kennedy and others 2007; Kennedy and others 2010). LandTrendr is a technique that employs a set of segmentation algorithms to identify salient trends and events in an annual time-series of Landsat imagery at the pixel scale. After accounting for large fires with MTBS, we extracted all abrupt, high-magnitude LandTrendr disturbances (1-2 year duration) and assumed these were stand-replacing

harvests. We also used LandTrendr data to fill in high-, moderate-, and low-severity fire pixels within MTBS non-processing mask areas (defined in Table A3; 7% of Metolius fire extents). In these areas, we extracted LandTrendr disturbances from the same time period as the fires and classified high, moderate, and low severity with LandTrendr relative change magnitudes of 50-100%, 30-50%, and 15-30%, respectively, based on comparisons in adjacent areas where MTBS severity was classified (data not shown).

For disturbances prior to 1985, we used an age map derived from regression models of Landsat spectral indices and georeferenced FIA plot data (Cohen and others 1995; Duane and others 2010). We aggregated this continuous age surface into six age classes (30, 50, 70, 80, 150, 250) to reduce the number of cover type by age class combinations in each 1 km cell. Deciduous pixels were assigned an age of 50 years based on the mean age of FIA plots in the region (Hudiburg and others 2009), and juniper woodlands were assigned an age of 70 years because many juniper stands in eastern Oregon originated following heavy grazing and fire exclusion between the late 19th Century and mid 20th Century (Gedney and others 1999). In addition, because fire exclusion co-occurred with widespread logging (for example, Hessburg and Agee 2003; Everett and others 2007), we assumed that forest pixels 75 years old or less originated as clearcut harvest and older pixels as stand-replacing fire. When only one disturbance occurred since 1985, we assumed that the stand age at the time of disturbance was 200 years (based on FIA plot ages in the region; Hudiburg and others 2009).

Table A1. Ecophysiological Parameters for Biome-BGC Simulation in East Cascades Ecoregion

Parameter	Unit	Value
Annual turnover rates		
Leaves and fine roots	$year^{-1}$	0.25
Live wood	$year^{-1}$	0.7
Whole plant mortality (MORT)	$year^{-1}$	0.02
Allocation ratios		
Fine root C/leaf C	DIM	1.3
Stem C/leaf C	DIM	2.2
Live wood C/total wood C	DIM	0.071
Coarse Root C/Stem C	DIM	0.25
Growth C/storage C	DIM	0.5
C/N ratios		
C/N of leaves	DIM	52
C/N of falling leaf litter	DIM	93
C/N of fine roots	DIM	58
C/N of live wood	DIM	50
C/N of dead wood	DIM	729
Leaf litter proportions		
Labile proportion	DIM	0.32
Cellulose proportion	DIM	0.44
Lignin proportion	DIM	0.24
Fine roots proportions		
Fine root labile proportion	DIM	0.32
Fine root cellulose proportion	DIM	0.44
Fine root lignin proportion	DIM	0.24

Dead wood proportions and lag terms		
Cellulose proportion	DIM	0.76
Lignin proportion	DIM	0.24
Time lag as snag	Year	1
Snag fall exponential decay constant	DIM	0.1
Canopy parameters		
Water interception coefficient	$LAI^{-1}\ d^{-1}$	0.041
Light extinction coefficient	DIM	0.5
Average specific leaf area	$m^2 kg^{-1}$ C	8.7
Ratio of sunlit to shaded LAI	DIM	1
Fraction of leaf N in Rubisco (FLNR)	DIM	0.035
Conductance parameters		
Maximum stomatal conductance	$m\ s^{-1}$	0.0015
Cuticular conductance	$m\ s^{-1}$	0.00001
Boundary layer conductance	$m\ s^{-1}$	0.08
Boundaries for conduction reduction		
Leaf water potential: start of reduction	MPa	-0.7
Leaf water potential: complete reduction	MPa	-2.5
VPD: start of reduction	Pa	1000
VPD: complete reduction	Pa	3500

Notes:

Based on Table A1 in Turner and others (2007). Values shown for evergreen needleleaf vegetation only (the cover type across most of the simulation landscape; Figure 1). Definitions: NA: DIM: dimensionless. For Cascade Crest Ecoregion, all values identical except MORT = 0.015 and FLNR = 0.04 (see optimization procedure in Appendix A).

Table A2. Combustion Factors for Pyrogenic Carbon Emissions Estimates.

Burn severity	Live stem	Foliage[1]	Dead stem	Forest floor[2]	Down woody detritus[3]
Low	0.02	0.125	0.11	0.66	0.17
Moderate	0.03	0.500	0.14	0.66	0.22
High	0.05	1.000	0.18	1.00	0.39

Notes:

Proportions are mean combustion factors, weighted by severity class area, derived from field-measurements in western Oregon conifer forests (Campbell and others 2007), except foliage.

[1] Foliage proportion from MTBS (http://mtbs.gov) burn severity classes for percent tree mortality (Table A3), which represents the transfer from live to dead tree pools.

[2] Weighted mean of litter and duff.

[3] Weighted mean of coarse and fine down woody detritus.

Due to model logic, live fine and coarse roots incur same effects as foliage and live stem, respectively.

Table A3. Monitoring Trends in Burn Severity (MTBS) Classification.

MTBS class	MTBS description[1]	Tree mortality % used in Biome-BGC modeling
Unburned to low severity ("Unburned/low" in text)	within fire perimeter, but either unburned, or visible fire effects occupy <5% of area	na[3]
Low severity[2]	all strata altered from prefire state; some strata substantially altered (particularly forest floor and understory vegetation); overstory mortality up to 25%	12.5
Moderate severity[2]	transitional in magnitude and/or uniformity between low- and high-severity; many possible combinations of diverse fire effects	50
High severity[2]	uniformly extreme, generally long-lasting effects across strata; overstory tree mortality typically >75%; understory vegetation and forest floor mostly consumed; >50% newly exposed mineral soil	100[4]
Increased greenness	fire-induced increase in vegetation cover, density, and/or productivity (usually herbaceous or shrub)	na
Non-processing mask	missing data due to sensor problems or interference (clouds, smoke, shadow, snow) or other geologic features such as water; filled in with LandTrendr data for Biome-BGC simulation	na

Notes:

Source: Schwind 2008, http://mtbs.gov

[1] Based on forested sites in general.

[2] Classes used in this study; other classes assumed unburned.

3 For sensitivity analysis, low-severity value (12.5%) used for unburned to low severity class.

[4] Proportional mortality close to 100% (such as 87.5%, the analog to low-severity 12.5%) was not possible due to model logic.

Figure A1. Example Biome-BGC simulation of low-, moderate-, and high-severity fire effects on annual NEP, based on mortality thresholds from MTBS (Table A3) and carbon pool-specific combustion factors (Table A2; Campbell and others 2007). Simulation runs from a representative ponderosa pine site with fire occurring in 1950, an arbitrary year that provides a reference for model behavior several decades following fire.

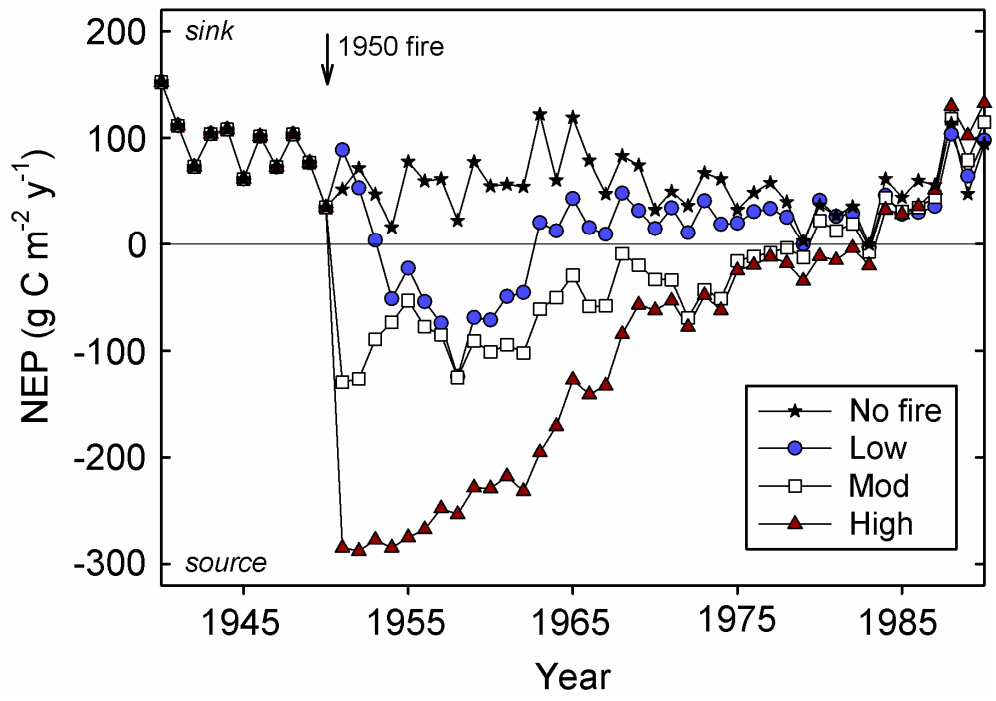

Appendix B. Figure B1. Fire extent and severity distribution across Oregon ecoregions, 2002-2003. Burn severity classes from MTBS (http://mtbs.gov). Forested ecoregions shaded gray. Ecoregion and MTBS classification described in methods section. Combined with the Biscuit Fire, the Metolius fires in this study accounted for the majority of fire extent during these 2 years (54% of fire extent across Oregon, 63% of fire extent within forested ecoregions). Across Oregon, 2002 was the most extreme fire year on record (1984-2005), whereas 2003 was an average fire year (determined from MTBS dataset). Spatial grain: 25 m. Projection: Universal Transverse Mercator NAD83.

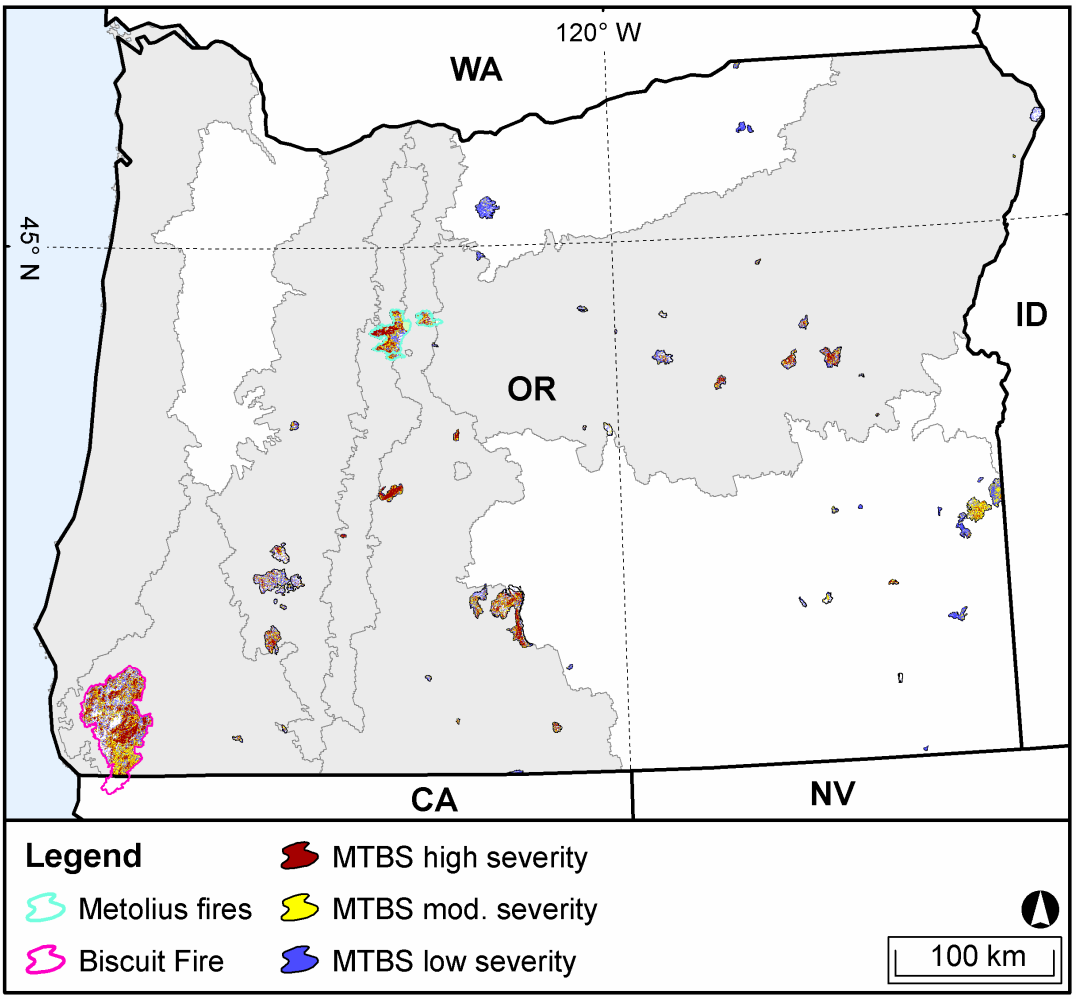

References Not Cited in Main Manuscript

Cohen WB, Spies TA, Fiorella M. 1995. Estimating the age and structure of forests in a multi-ownership landscape of western Oregon, USA. Int J Remote Sens 16:721–46.

CONUS. 2009. Conterminous United States multi-layer soil characteristics dataset for regional climate and hydrology modeling. http://www.soilinfo.psu.edu/index.cgi?index.html.

Everett R, Baumgartner D, Ohlson P, Schellhaas R, Harrod R. 2007. Development of current stand structure in dry fir-pine forests of eastern Washington. J Torrey Bot Soc 134:199–214.

Gedney DR, Azuma DL, Bolsinger CL, McKay N. 1999. Western Juniper in Eastern Oregon. USDA Forest Service General Technical Report PNW-GTR-464. OR: Portland.

Hessburg PF, Agee JK. 2003. An environmental narrative of Inland Northwest United States forests, 1800–2000. For Ecol Manag 178:23–59.

Thornton PE, Running SW, White MA. 1997. Generating surfaces of daily meteorological variables over large regions of complex terrain. J Hydrol 190:214–51.